ELSEVIER

Journal of Fluorine Chemistry 82 (1997) 85–90

JOURNAL OF FLUORINE CHEMISTRY

Electron beam induced degradation of polyperfluorinated ethers: $-(CF(CF_3)-CF_2-O)_n-$, for $n=4$, 8 and 50

J. Pacansky, R.J. Waltman, D. Jebens, O. Heery

IBM Almaden Research Center, 650 Harry Road, San Jose, CA 95120-6099, USA

Received 27 June 1996; accepted 21 August 1996

Abstract

Polyperfluorinated propylene oxides, $-(CF(CF_3)-CF_2O-)_n-$, where $n=4$, 8 and 50, are exposed to electron beams and their subsequent degradation monitored via infrared spectroscopy at $T=11$ and 298 K. COF_2, CF_4, and R–CFO are produced and their G values are reported as a function of n, the number of monomer units, in the polymer. The G values range from 0.1 to 3, depending upon the gas product and n. The efficiency for gas evolution decreases with increasing number of monomer units. For $n=4$, R–CFO, CF_4 and COF_2 are produced with G values of 3.0, 2.7, and 2.4, respectively. As n increases to 50, COF_2 becomes the dominant product with a G value of 1.0, followed by CF_4 at 0.7, and R–CFO at 0.1.

Keywords: Perfluorinated ether; Lubricant; Electron beam; Degradation; G value

1. Introduction

Polyperfluoroether liquids have widespread applications as industrial lubricants [1–7] because of their intrinsic stability to temperature and chemical attack. Additionally, they exhibit a relatively small intrinsic temperature dependence on viscosity and low vapor pressures, making these materials ideal for use in drastic environments. However, a scission in the polymer chain can cause the chemical and physical properties to change rather dramatically. for example, β-cleavage reactions initiated by radicals can cause mass loss, decrease in viscosity, the formation of reactive oligomers containing –CFO end groups, and evolution of reactive gases such as COF_2 and CF_3CFO. Consequently, thermally [8,9] and radiation [10–14] induced degradation studies on polyperfluorinated ethers continue to be an active area of investigation.

In this report we continue our studies on the mechanism(s) of polyperfluoroether degradation induced by electron beams. We have established from previous studies [10–14] the following reaction sequence:

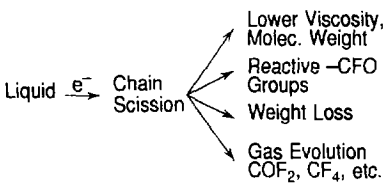

Here the G values for main chain degradation as a function of chain length are reported for the polyperfluoropropylene oxide structures:

$$CF_3CF_2O-(CF(CF_3)-CF_2O-)_n-CF_2CF_3$$

where $n=4$, 8 and 50. The G value is defined as the number of molecules formed or decomposed per 100 eV of absorbed energy. The repeating monomeric unit is $-(CF(CF_3)-CF_2O-)_n-$, i.e. polyperfluoropropylene oxide, or PPFPO. We use the acronyms PPFPO-4, PPFPO-8 and PPFPO-50 to distinguish the different materials.

2. Experimental section

2.1. Materials

PPFPO-4, PPFPO-8 and PPFPO-50 were obtained from E.I. DuPont De Nemours and Company (Delaware) under the tradenames Krytox TLF-6082, Krytox TLF-6217 and Krytox 16256, respectively. The number average molecular weight of the polymer, PPFPO-50, is $M_n=8500$, and the density is $\rho=1.951$. The densities of PPFPO-4 and PPFPO-8 are 1.83 and 1.88 g cm^{-3}, respectively, as measured with a pycnometer at 22 °C.

PII S0022-1139(96)03533-6

2.2. Electron beam exposure tools

Electron beam exposures of the polyperfluoroether samples under 1 atm pressure and room temperature were achieved using a CB 150 Electron Processor (Energy Sciences, Inc., Woburn, MA) which allowed exposures of the samples to a 102 kV electron beam in an atmosphere of nitrogen. A description of the electron beam exposure tools has been given elsewhere [12]. The gases produced from the electron beam exposure of the poly(perfluoroethers) were collected in a stainless steel chamber with KBr windows to allow infrared interrogation. Complete descriptions of the gas cell and methodology, and dosimetry have been disclosed in an earlier publication [12].

The apparatus used for the 25 kV electron beam exposure to the samples under vacuum and at low temperatures has also been described [13]. The electron beam-induced changes in the samples were followed using IR specular reflection spectroscopy, using a Perkin Elmer 580 IR Spectrometer equipped with a Model 3600 Data Station. For these purposes, the polyperfluoroethers were spin coated onto Au substrates to thicknesses of 1.0 μm, well below the Grün range, R_G, of 7 μm, to ensure complete electron beam penetration into the samples. The Grün range is the maximum depth to which energy is dissipated in a material by the electron beam [15]. The reflectivity measurements were made in situ by rotation of the sample from the electron beam to the IR beam. All measurements were made with the incident IR beam at 25° from normal to the sample plane. For the perfluorinated ether film, and film thicknesses studied herein, we have determined that an incident charge density, Q, of 10 $\mu C\ cm^{-2}$, corresponds to an absorbed dose of 2.3 Mrad.

3. Computational details

All calculations were performed using the *Mulliken* computer code [16], using IBM RISC 6000 computers. Hartree–Fock calculations were performed using restricted wavefunctions and the polarized 6-31G* basis set [17]. Harmonic vibrational frequencies were calculated by differentiation of the energy gradient at the optimized geometries; no imaginary frequencies were computed.

4. Results and discussion

4.1. Low temperature irradiation

The infrared spectrum of PPFPO-4 before and after electron beam exposure at $T = 11$ K under vacuum is shown in Fig. 1 as an illustrative example. The low temperature electron beam irradiation of PPFPO-8 and PPFPO-50 produce similar results; consequently, their analyses are covered here in the discussion of PPFPO-4. The initial spectrum before electron beam exposure shows rather broad absorption bands

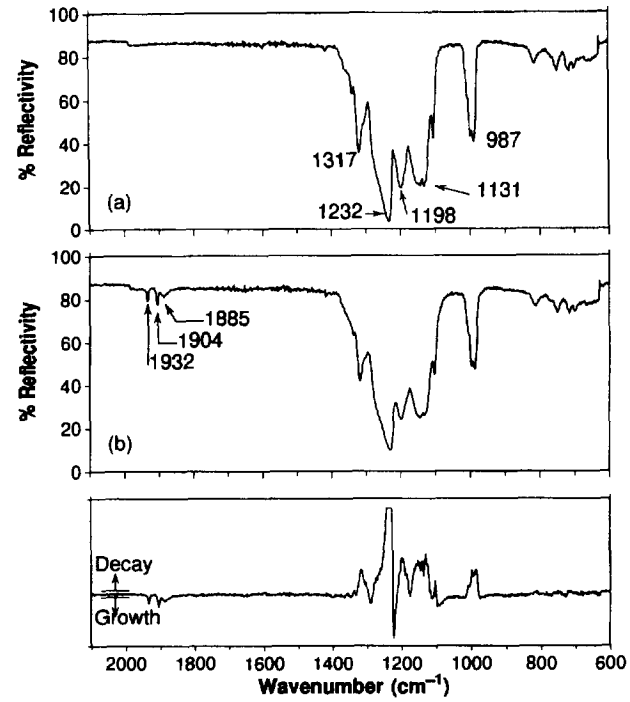

Fig. 1. Specular reflection infrared spectrum of PPFPO-4 before and after exposure to a 25 kV electron beam at $T = 11$ K: (a) 0; (b) 15 $\mu C\ cm^{-2}$. A difference spectrum is presented in (c).

in the 1400–1100 cm^{-1} region characteristic for these perfluorinated materials. Based upon extensive ab initio theoretical studies on these types of materials [18], the characteristic bands in PPFPO-4 are identified as follows: the band at 1317 cm^{-1} is attributed to a mixture of main chain CC, CF_2 and CF_3 stretching vibrations. The intense band centered at 1232 is attributed to a mixture of CF_2 and CC stretching modes involving the pendant carbon atom, with contributions from the CF stretches in the CF_3 end groups. The absorption band at 1198 cm^{-1} is primarily attributed to CF stretches involving the pendant CF_3 group. The bands centered at 1142 and 1131 cm^{-1} are attributed to the CO stretch of the ether group. The isolated band centered at 987 cm^{-1} is characteristic of the PPFPO main chain architecture, involving CC vibrations between the main chain and pendant CF_3 carbon atom, and CF_3 and CF_2 stretching modes as well.

After an incident exposure of 15 $\mu C\ cm^{-2}$ (34 Mrad), the major changes observed in the infrared spectrum of PPFPO-4 are evolution of new bands in the 1950–1880 cm^{-1} region. The difference spectrum between Fig. 1(a) and Fig. 1(b) is more revealing, and is presented in Fig. 1(c) to highlight the fact that considerable changes have taken place in PPFPO-4 as a result of the electron beam irradiation, even at 11 K. The formation of the new bands are observed at 1932, 1904 and 1885 cm^{-1}, characteristic of C=O stretching modes in carbonyl fluorides. The 1932 and 1904 cm^{-1} bands are attributed to the carbonyl fluoride C=O stretch and symmetric C–F stretch in strong Fermi resonance with each other [19]. The 1885 cm^{-1} vibration is from an acid fluoride –CFO residing on the end of a broken chain [11]. Concomitant with the

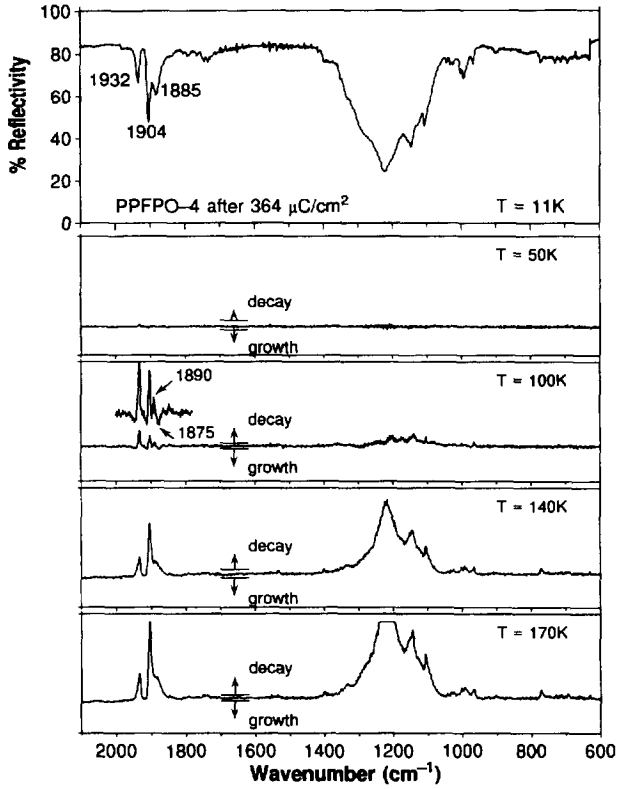

Fig. 2. (a) Specular reflection infrared spectrum of PPFPO-4 after exposure to a 25 kV electron beam of incident charge density 364 μC cm^{-2} at T= 11 K. The figures beneath present the warm up difference spectra as a function of temperature.

formation of the new bands are significant changes in the infrared bands in the 1400–950 cm^{-1} region. These changes may result from very low molecular weight fragments that are pumped away by the vacuum system, or simply scissioned fragments relaxing to a lower energy configuration.

In an effort to observe additional changes in the infrared spectrum of PPFPO-4, the sample was irradiated to doses of up to 364 μC cm^{-2} (837 Mrad); these data are presented in Fig. 2. After exposure of the material to such a large dose, considerable damage to the polyperfluoroether is observed. This is consistent with data obtained previously from the electron beam irradiation of polyperfluorinated ether liquids at room temperature, where it is observed that exposures to similarly large doses cause mass loss of up to ≈80% [14]. Here, as shown in the infrared spectrum at T= 11 K, much of the fine structure in PPFPO-4 observed prior to irradiation (Fig. 1(a)) is now replaced by a rather broad and featureless absorption band in the 1400–1000 cm^{-1} region. After irradiation, the relatively intense band at 987 cm^{-1} is significantly depleted, and intense carbonyl absorptions are instead observed in the 1900 cm^{-1} region. The irradiated perfluorinated ether samples were then gradually warmed from 11 K to room temperature. The warm-up spectra, Fig. 2(b)–(e), are presented as a series of difference spectra between the infrared spectrum recorded at the specified temperature in the figure and in the infrared spectrum at 11 K. At 50 K, no products volatile enough to be pumped away by the vacuum system are observed. At T= 100 K, the –CFO carbonyl absorption centered near 1900 cm^{-1}, together with the broad absorption region between 1400–1050 cm^{-1}, begin to be pumped away by the vacuum system. What is interesting and significant here is that the warm-up reveals the presence of at least two infrared absorption bands that make up the 1885 cm^{-1} band in PPFPO-4. The entity giving rise to the higher frequency 1890 cm^{-1} infrared absorption band is apparently volatile enough to be pumped away at this temperature and is suggestive of CF_3CFO. The other, at 1875 cm^{-1}, persists in bulk and is not pumped away until the sample is elevated to a higher temperature, suggesting its occurrence as an end group of a broken chain, i.e. an oligomer R–CFO with R > CF_3–. Upon continued warming of the irradiated sample to T= 140 and 170 K, all volatile components and fragments begin to relax and/or be pumped away by the vacuum system as shown in Fig. 2(d), (e). The same trend is observed until at T= 298 K virtually all of the material is pumped away from the gold substrate. Similar change sin the infrared spectra of PPFPO-8 were observed, while for PPFPO-50, by virtue of its much higher molecular weight and hence, lower vapor pressure, more residual material remained on the gold substrate after similar treatment as compared to PPFPO-4 and PPFPO-8.

In summary, the infrared analyses of electron beam irradiated PPFPOs at low temperature and subsequent warm-up indicate that COF_2 and R–CFO products are formed. The warm-up spectra indicates that several R–CFO entities are present.

4.2. Room temperature irradiation

To identify the volatile fragments lost from PPFPO-4, PPFPO-8 and PPFPO-50, the gases generated by irradiation of the polyperfluoroether liquids at room temperature were collected in an infrared cell as a function of absorbed dose. It was observed previously [14] that electron beam exposure of liquid PPFPO-50 at room temperature produce COF_2, CF_4, and CF_3CFO, that could be detected in the gas phase. Concomitantly, an infrared band at 1885 cm^{-1} developed in the irradiated liquid which persisted in the liquid as long as moisture was excluded to prevent hydrolysis to R–COOH. Based upon these observations, the 1885 cm^{-1} absorption was attributed to the formation of –CFO end groups on the main chain, i.e. they were oligomers with –CFO end groups [11,14]. The results of identical experiments conducted on PPFPO-4 and PPFPO-8 are contained in the infrared spectra presented in Fig. 3, along with the results for PPFPO-50 as reference. In all cases, COF_2 is identified by its characteristic stretching vibrations at 1957, 1931 cm^{-1} (C=O stretch) and at 1255, 1232 cm^{-1} (asymmetric C–F stretch) [19], and as compared to authentic gas. The band centered at 1278 cm^{-1} is unequivocally identified as the C–F stretching vibration in CF_4, as compared to the authentic gas. The shoulder at 1897 cm^{-1}, together with 1332 and 1098 cm^{-1} is characteristic of CF_3CFO [12]. The absorption band at 668 cm^{-1} is

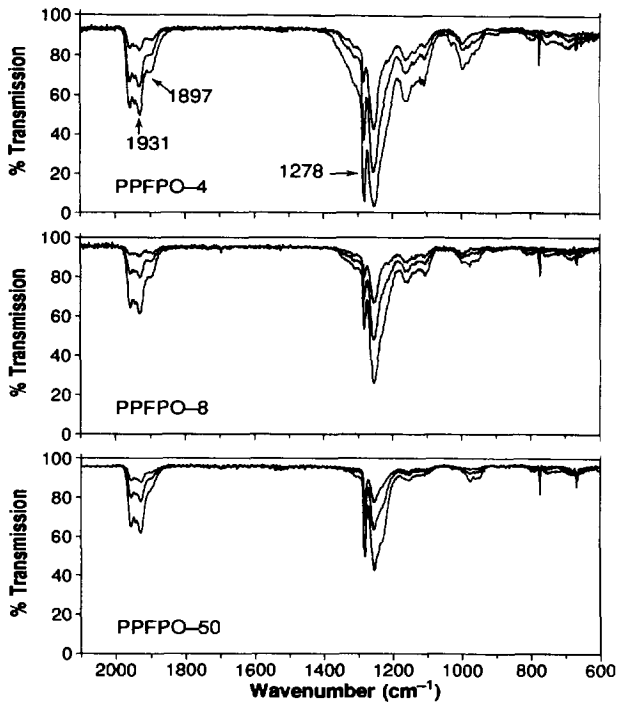

Fig. 3. Gas phase transmission infrared spectra of PPFPO-4, PPFPO-8, and PPFPO-50 as a function of absorbed dose at room temperature: 15, 31 and 62 Mrad.

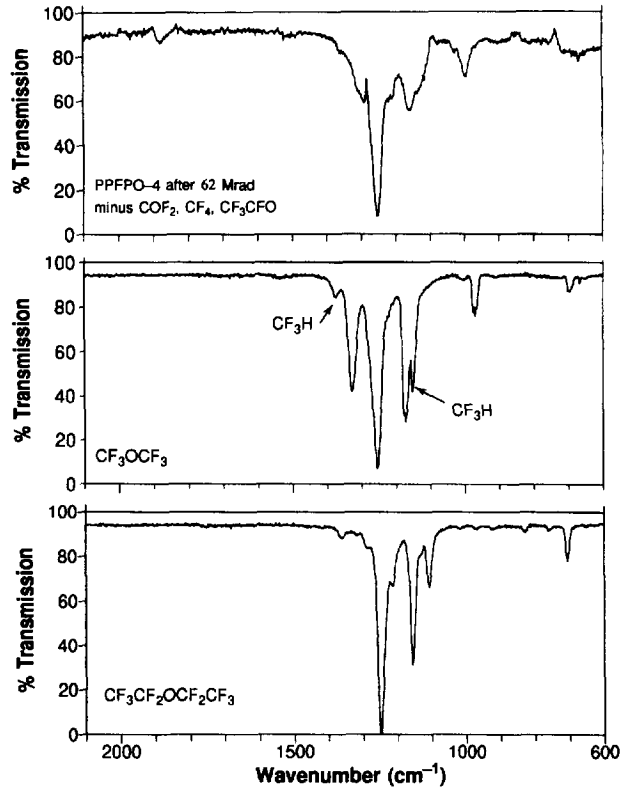

Fig. 4. (Top) PPFPO-4 after 62 Mrad minus some known gas products. (Middle) and (Bottom) Experimental spectra of perfluorinated ethers. In the middle spectrum, the CF_3H impurity is identified.

attributed to carbon dioxide, produced by irradiation of both PPFPO and its gaseous products COF_2 and R–CFO [12].

The major differences between the low molecular weight PPFPO-4 and -8, and PPFPO-50, are the much more intense infrared bands near 1161 and 1105 cm^{-1}, the more intense shoulder at 1897 cm^{-1}, and the more prominent background absorption between 1400–1000 cm^{-1} region. Since the monomeric units are identical and only the number of monomer units have decreased from PPFPO-50 to PPFPO-4, we conclude that these absorption bands are directly attributable to the participation of the CF_3CF_2O– end groups in gas phase product formation. Attempts to subtract out the infrared spectra of some known gases (COF_2, CF_3CFO, CF_4) from the experimental spectrum after 62 Mrad left the residual difference spectrum shown in Fig. 4. The band centers that are left in the gas phase product spectrum are suggestive of a small quantity of R–CFO (1880 cm^{-1}), and possibly simple ethers (1255, 1160 cm^{-1}) and perfluoroalkanes (1250, 1000 cm^{-1}); however, no definitive assignments are possible based upon infrared spectra alone. However, for comparison, the infrared spectra of perfluorodimethyl- and perfluorodiethyl-ethers are also presented in Fig. 4. The general shapes of the infrared spectra of simple ethers appear to match major portions of the residual spectrum in Fig. 4 (top).

A comparison of the G values for formation of the various gases are summarized in Fig. 5. The methodology for calculating G values from infrared measurements has been outlined previously [14]. Briefly, a plot of the changes in the integrated absorbance ($\int \log(T_0/T)\, d\nu$) versus absorbed dose is related to changes in the number of molecules formed or destroyed per absorbed dose. The integrated absorbance is related to the number of molecules via the integrated molar absorption coefficient B, which has been reported for COF_2, CF_4, and CF_3CFO gases [12]. We note here that the integrated molar absorption coefficient B for CF_3CFO was used to determine the G value for evolution of the 1987 cm^{-1} R–CFO band in Fig. 3. As shown in Fig. 5, the G values for formation of gaseous COF_2, R–CFO, and CF_4 vary from ≈ 0.1 to 3 as a function of monomer unit chain length and, in all cases, decrease with increasing chain length. For COF_2 and CF_4 evolution, the dependence is rather modest, and only an approximately twofold increase in the G values is observed. For R–CFO, the increase in G value with de-

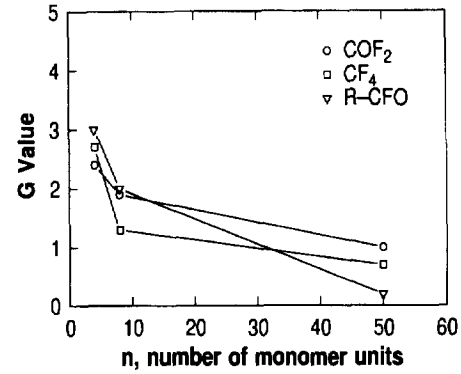

Fig. 5. The G values for formation of gases as a function of the number of monomer units.

Table 1
HF/6-31G* computed reactions from radicals **I** and **II** (see below)

CF_3CF_2O–$CF_2CF(CF_3)O$–$CF_2CF(CF_3)$–···–O–···–CF_2–$CF(CF_3)O$–$CF_2CF(CF_3)O$–CF_2CF_3

PPFPO-4

↓

$CF_3CF_2OCF_2CF(CF_3)OCF_2CF(CF_3)OCF_2^{\bullet}$ + $^{\bullet}CF(CF_3)OCF_2CF(CF_3)OCF_2CF_3$

I II

Reaction	ΔH (kcal mol^{-1})
I → $CF_3CF_2OCF_2CF(CF_3)OCF_2CF(CF_3)^{\bullet}$ (**III**) + COF_2	−2.00
II → $CF_3CFO + {}^{\bullet}CF_2CF(CF_3)OCF_2CF_3$	+2.88
III → $CF_3CF_2OCF_2CF(CF_3)O^{\bullet}$ (**IV**) + $CF_2{=}CFCF_3$	+32.07
IV → $CF_3CF_2OCF_2CFO + CF_3^{\bullet}$	+6.23
IV → $CF_3CF_2OCF_2^{\bullet}$ (**V**) + CF_3CFO	+4.93
V → $CF_3CF_2^{\bullet} + COF_2$	+0.49

creasing chain length in considerably more dramatic, from 0.1 to 3. Hence when $n = 4$, R–CFO is the predominant product (Fig. 5) while for $n = 50$, COF_2 predominates. Since the monomer unit is the same for all three PPFPOs, the data suggests that there is a greater proportion of products originating from the CF_3CF_2O– end groups that somehow translates into R–CFO evolution. These aspects will be considered below. For now, we note that a G value of 1 for COF_2 evolution from the polymer PPFPO-50, is substantially less than evolution from unbranched perfluorinated ethers where G values as high as 8 have been measured [14]. The improved resistance to COF_2 evolution is attributed to the pendant –CF_3 units that allow alternative radiation-induced degradation pathways such as evolution of CF_4.

The formation of the gas phase products from the electron beam irradiation of PPFPO are now considered using ab initio theory. Barnaba et al. [10], in his studies of irradiated poly(tetrafluoroethylene oxide), found two carbon-centered radicals and one oxygen-centered radical, one of the carbon-centered radicals being most stable. Hence, we consider the scission of both the C–C and C–O bonds in PFFPO (Table 1) based upon the products observed in the infrared spectra (Figs. 2 and 3). The bond dissociation energies for C–O and C–C cleavage [20] at 298 K are 73 and 75 kcal mol^{-1}, respectively, thus the energy requirement is slightly less for a C–O scission. Consider first the reaction scheme presented in Table 1. Due to the large size of the PPFPO-4 molecule, ab initio calculations using reasonably flexible basis sets were prohibitive. Therefore, to obtain reliable computational data, only those reactions arising from fragments after an initial main chain scission were considered. The starting fragments were radicals $CF_3CF_2OCF_2CF(CF_3)OCF_2CF(CF_3)OCF_2^{\bullet}$, **I**, and $^{\bullet}CF(CF_3)OCF_2CF(CF_3)OCF_2CF_3$, **II**, arising from an initial C–C cleavage. As summarized in Table 1, a β-scission of **I** to produce COF_2 and radical III (see Table 1) is predicted to be exothermic with a ΔH of −2.0 kcal mol^{-1}. As consistently observed [21], evolution of COF_2 proceeds with a small ΔH and is usually the predominant gas phase product obtained from the scission of polyperfluorinated ether polymers. From the radical **II**, CF_3CFO is produced from a β-cleavage of the C–O bond, computed to be endothermic with a $\Delta H = +2.9$ kcal mol^{-1}. This corroborates the observed preferential production of COF_2 relative to CF_3CFO from the main chain scission of PPFPO-50 since CF_3CFO must be here generated from the main chain. Let us now consider radical **III**, $CF_3CF_2OCF_2CF(CF_3)OCF_2CF(CF_3)^{\bullet}$, obtained from the β-cleavage of COF_2 from **I**. A β-cleavage of **III** would ostensibly produce radical **IV**, $CF_3CF_2OCF_2CF(CF_3)O^{\bullet}$, and $CF_3CF{=}CF_2$. The computed $\Delta H = 32.1$ kcal mol^{-1}, is significantly more endothermic than the β-cleavage reactions that produce perfluoroaldehydes. A signature for such a reaction is the formation of $CF_3CF{=}CF_2$ which would normally exhibit a characteristic infrared absorption band at 1790 cm^{-1} attributed to a C=C stretching mode [22]. Since this infrared absorption band was not observed experimentally (Figs. 2 and 3) this reaction was precluded.

Radical **IV** may be considered to arise from either **III** as shown in Table 1, or from a direct C–O bond scission in PPFPO-4 that occurs between a primary carbon atom (–CF_2–) bonded to an oxygen atom. Radical **IV** may follow one of two reaction coordinates based upon a β-scission scheme; first, it may eliminate CF_3CFO and produce radical **V**, $CF_3CF_2OCF_2^{\bullet}$, with a ΔH of +4.9 kcal mol^{-1}, or second, it may eliminate $CF_3^{\bullet}$ and produce $CF_3CF_2OCF_2CFO$ with a ΔH of +6.2 kcal mol^{-1}. Since the ΔH for either reaction is similar, they may occur competitively. Since the elimination of $CF_3^{\bullet}$ is possibly an important source for subsequent CF_4 formation, as observed in Fig. 3, then $CF_3CF_2OCF_2CFO$ may be a viable product also. The $CF_3CF_2OCF_2CFO$ would simultaneously account for both the presence of an ether linkage and the –CFO group. Since it necessarily involves the end group, its presence would explain the more prominent absorption bands for PPFPO-4 (and -8) in Fig. 3.

To provide additional corroboration for the identity of the gas phase products (Fig. 3) ab initio computed gas phase spectra are shown for some gas products in Fig. 6. When Fig. 6 (middle) is compared with Fig. 3 (top), we observe that many of the experimental band centers developed in the experiment are reproduced by COF_2, CF_4 and CF_3CFO. In Fig. 6 (top), the computed infrared spectra of an oligomeric R–CFO is shown and in Fig. 6 (bottom), that of $CF_3CF{=}CF_2$ is provided. The occurrence of the 1155 cm^{-1} band in both Fig. 3 (top) and 6 (top), a perfluorinated ether C–O stretching mode, provides corroboration that the R group in R–CFO may be something like $CF_3CF_2OCF_2$–, in addition to the simple CF_3. Fig. 6 (bottom) provides evidence that β-scission reactions leading to perfluoroalkenes are not observed in the gas phase due to the absence of an identifying band at near 1790 cm^{-1}.

Finally, we note that the reaction of $F^{\bullet}$ with any of the radical species that we have considered in Table 1 will produce molecules such as CF_4, C_2F_6, $CF_3CF_2OCF_3$, etc., which

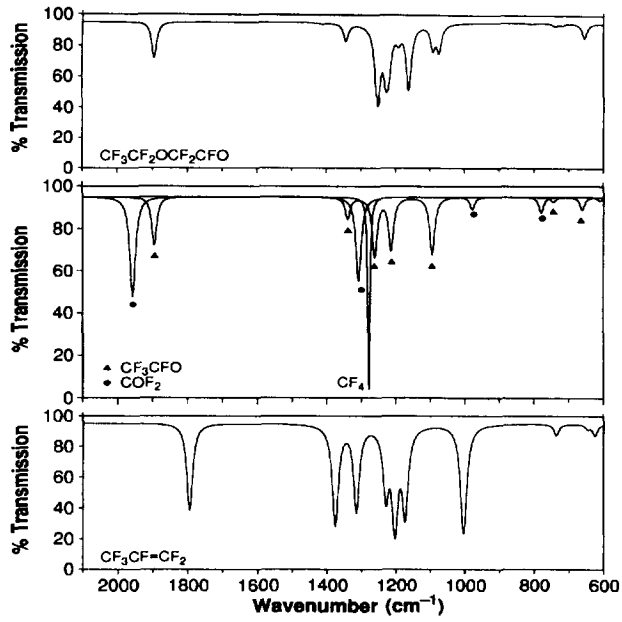

Fig. 6. HF/6-31G* computed infrared spectra.

generally satisfy many of the infrared bands observed in Fig. 3.

5. Summary

The electron beam induced decomposition of PPFPO liquids, $-(CF(CF_3)-CF_2O-)_n-$, where $n=4$, 8 and 50, produces COF_2, CF_4, and R–CFO. Both low temperature and gas phase infrared spectra identify the presence of several entities that give rise to R–CFO. When the molecular weight is high, PPFPO-50, COF_2 is the major gaseous species that is collected and products containing the R–CFO end group are largely oligomeric and hence, are observed to remain in the bulk liquid [11,14]. When the molecular weight is low, PPFPO-4, the "oligomers" containing the –CFO end groups are much smaller and as a consequence, have much higher vapor pressures [13] leading to more ready evolution into the gas phase. The gaseous products containing the end groups may contain the ether (1161 cm^{-1}) functional moiety, attributed to the $CF_3CF_2OCF_2-$ structure. Such infrared bands were observed more efficiently in PPFPO-4 compared to PPFPO-50.

The G values for formation of all gas phase products increase with decreasing number of monomer units. This is attributed to the proportionately smaller residual chain after scission, having a comparatively lower vapor pressure [13]. For small n, e.g. $n=4$, R–CFO products predominate while for larger n, e.g. $n=50$, COF_2 predominates. The efficiency for formation of gaseous R–CFO falls dramatically for large n, indicating that the CF_3CF_2O- end groups are participatory.

References

[1] D. Sianesi, V. Zamboni, R. Fontanelli and M. Binaghi, *Wear, 18* (1971) 85.
[2] J.C. Devins, *Natl. Acad. Sci. NRC Annu. Rep.*, (1977) 398.
[3] A. Luches and L. Provenzano, *J. Phys. D.: Appl. Phys., 10* (1977) 339.
[4] L. Holland, L. Laurenson and P.N. Baker, *Vacuum, 22* (1972) 315.
[5] J. Hennings and H. Lotz, *Vacuum, 27* (1977) 171.
[6] L. Laurenson, N.T.M. Dennis and J. Newton, *Vacuum, 29* (1979) 433.
[7] T.R. Bierschenk, H. Kawa, T.J. Juhlke and R.J. Lagow, *NASA CR-182155* 1988.
[8] P.H. Kasai, W.T. Tang and P. Wheeler, *Appl. Surf. Sci., 51* (1991) 201.
[9] P.H. Kasai, *Macromolecules, 25* (1992) 6791.
[10] P. Barnaba, D. Cordischi, A. Delle Site and A. Mele, *J. Chem. Phys., 44* (1966) 3672.
[11] J. Pacansky, R.J. Waltman and C. Wang, *J. Fluor. Chem., 32* (1986) 283.
[12] J. Pacansky and R.J. Waltman, *J. Phys. Chem., 95* (1991) 1512.
[13] J. Pacansky, R.J. Waltman and M. Maier, *J. Phys. Chem., 91* (1987) 1225.
[14] J. Pacansky and R.J. Waltman, *Chem. Mater., 5* (1993) 486.
[15] A.E. Grün, *Z. Naturforsch., 12A* (1957) 89.
[16] J.E. Rice, H. Horn, B.H. Lengsfield, A.D. McLean, J.T. Carter, E.S. Replogle, L.A. Barnes, S.A. Maluendes, G.C. Lie, M. Gutowski, W.E. Rudge, S.P.A. Sauer, R. Lindh, K. Andersson, T.S. Chevalier, P.-O. Widmark, D. Bouzida, G. Pacansky, K. Singh, C.J. Gillan, P. Carnevali, W.C. Swope and B. Liu, *Mulliken*, Almaden Research Center, IBM Research Division, 6500 Harry Road, San Jose, CA 95120-6099, USA.
[17] K. Raghavachari and J.A. Pople, *Int. J. Quant. Chem., 20* (1981) 1067.
[18] J. Pacansky, M. Miller, W. Hatton B. Liu and A. Schiener, *J. Am. Chem. Soc., 113* (1991) 329.
[19] (a) J. Pacansky, R.J. Waltman and Y. Ellinger, *J. Phys. Chem., 98* (1994) 4787; (b) P.D. Mallison, D.C. McKean, J.H. Holloway and I.A. Oxton, *Spectrochim. Acta, 31A* (1975) 143.
[20] J. Pacansky and R.J. Waltman, unpublished data.
[21] J. Pacansky, R.J. Waltman and G. Pacansky, *Chem. Mater., 5* (1993) 1526.
[22] U. Groß, P. Dietrich, G. Engler, D. Prescher and J. Schulze, *J. Fluor. Chem., 20* (1981) 33.